

# Thermal Analysis of Ultrafine Wool Powder

Weilin Xu, Weiqi Guo, Wenbin Li

Wuhan Institute of Science and Technology, Wuhan 430073, People's Republic of China

Received 28 February 2002; accepted 11 July 2002

**ABSTRACT:** Wool powder was produced from wool fiber by pretreatment and then ground by a specially designed machine. Scanning electron micrograph (SEM) photos show that ultrafine wool powder around 2  $\mu\text{m}$  in diameter can be produced from fiber around 25  $\mu\text{m}$  in the diameter, and most of the powder is in the form of needles. The powder can be widely applied in new biomedical material development and cosmetic products. Thermal analysis of thermogravimetry (TG) and differential scanning calorimetry (DSC) show that the temperature for moisture evaporation in the powder was elevated to around 150°C from the control wool

fiber, which was around 120°C. As the powder particle size decreases, the temperature corresponding to the crystal cleavage and the destruction of the crosslinkages increased, which is perhaps mostly due to the new crosslinks and new crystal that were produced during powder processing. The temperature for the liquefaction was also elevated and the relative TG results show that the last residue of the powder after 600°C is higher than that of the control sample. The thermal results show that as the powder particle size decreases, the thermal stability increases slightly. © 2003 Wiley Periodicals, Inc. *J Appl Polym Sci* 87: 2372–2376, 2003

## INTRODUCTION

Silk and wool are high quality natural protein fibers that have been widely used as high quality textile material. However, as textile fibers they should have some special physical properties, such as a certain length. Sometimes there is some waste silk or wool fiber that cannot be used as a textile resource. So many researchers, especially in Japan, try to develop new applications for those fibers because their excellent intrinsic properties can be used to develop new materials in biotechnological and biomedical fields. In further study, moderate quantities of silks and silk-mimic biopolymers have been achieved due to advances in molecular biotechnology and protein engineering. However, 100% regenerated silk fiber has not been industrially produced because no proper spinning technology has come out.<sup>1,2</sup>

However, material properties depend not only on the macromolecule but also on the structure—the way the macromolecule is put together. So silk is widely produced in the form of powder by different methods.<sup>2–6</sup> Silk powder is easier to produce than the regeneration of its fiber. Silk fibroin powder has already found its utility as cosmetic materials and functional foods. Powdered silk fibroin is considered effective as

an additive for cosmetic and pharmaceutical preparations because of its moderate moisture absorption and retention properties, and its high affinity for human skin and silk; actually, wool powder also preserve these virtues. Silk powder is one of the useful physical forms of silk fibroin protein, as well as fiber and film, for biomaterial applications.<sup>7,8</sup> Silk powder is also applied in textile finishes. Taikyū Shoten K. K. has developed the technology to finish yarn-dyed cotton fabrics with silk powder and plans to market these cotton fabrics under the “Powder Taste” brand.<sup>9</sup> The fine silk powder is absorbed into the cotton fibers to create a soft hand. The fabric offers good drape characteristics as well as the moisture-absorbing properties inherent in cotton fabrics.

Usually, compared with inorganic fiber, polymer fibers not only have high strength but also high break intensity and high elongation. So they are very difficult to crush into a small powder. Moreover, even they are cut into short pieces, they still tend to wind together to form balls during grinding. In order to get fine silk powder, usually silk fibroin powders are produced by special chemical pretreatment to destroy the chemical bond and to reduce the crystallinity.<sup>5</sup> High energy irradiation is also used to destroy the crystal.<sup>4</sup> After pretreatment, silk fibroin fibers are dissolved into an aqueous calcium chloride solution at high temperature, followed by a dialysis treatment to remove the salt; this solution is dehydrated, dried, and pulverized to yield a fine fibroin powder.<sup>6–8</sup> Recently, simpler methods, which do not include dissolution and dialysis processes for silk fibroin, have been pro-

Correspondence to: W. Xu (Weilin\_xu@hotmail.com).

Contract grant sponsor: National Natural Science Foundation of China.

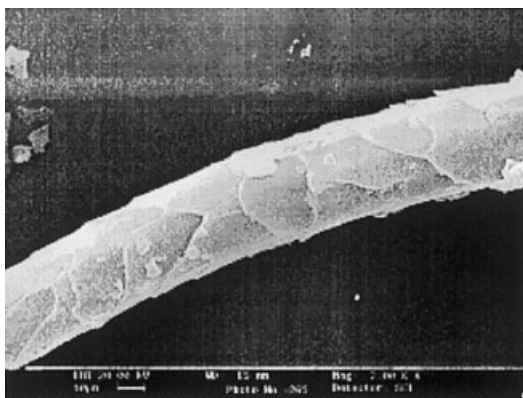


**Figure 1** Wool fiber ground for 5 min (single fiber—sample 1).

posed.<sup>9,10</sup> For example, a rotary blade mill was used to cut fibers with an average size of about 100  $\mu\text{m}$ . Then the roughly cut silk fibroin fibers were pulverized by a conventional ball mill. However, it took 12 h to produce the powder.

As for wool fiber, it is cheaper and friendly to the human skin; its strength is less than silk fiber. In order to develop new products from abundant wool fiber, some researchers are also trying to develop wool film to wrap products.<sup>10</sup> Due to their low price and availability, these films are more necessary to be developed into fine powder, especially for those unsuitable for the spinning of yarn, as they are small in diameter and their performance are very excellent than the longer and stronger fibers that are more welcome in the textile industry. Fine powders from wool fibers were produced by an explosive puffing treatment with saturated steam of unmodified and reduced wool fibers. It was found that the crystal content and the  $\alpha$ -helical structure were not affected by puffing.<sup>11</sup> In our research, we have developed a new method to produce fine wool powder. We report in this article on some results on the powder thermal properties.

## EXPERIMENTAL

The wool fiber was Australian wool provided by Mayer Corporation of Hubei. The diameter of the wool fiber was mostly around 25  $\mu\text{m}$ . The wool fiber was cut into short pieces around 3 mm, on a rotary blade. It was then pretreated by 0.5% NaClO solution at room temperature. After the excessive water was removed, the wool powder was ground between two mills that were made from special material. The mills have special properties such as very low heat generation and high anti-abrasion property. The fiber pieces could be easily crushed into small powder under the mechanical action including pressure, drawing, torsion, and shear action. For obtaining different wool powders of different sizes, different grinding times

were applied. We got four different samples: control sample (wool fiber, also named sample 0), sample 1, which was ground for 5 min; sample 2, which was crushed for 0.5 h; and sample 3, which was crushed for 3 h.

Scanning electron microscopy (SEM) analysis was carried out with a JAX-333S microscope, at 10 kV acceleration voltage, after gold coating.

Thermogravimetry (TG) was performed on the tester of TG 50, nitrogen protected, on TA processor of model Mettler TC11, at a heating rate of 20°C/min. Differential scanning calorimetry (DSC) was performed on model DSC25, on TA processor of model Mettler TC11, at a heating rate of 20°C/min. The open aluminum cell was swept with nitrogen gas during the analysis.

## RESULTS AND DISCUSSION

### SEM photos

Figure 1 shows that some of the scales on sample 1 is evidently clipped from the fiber; at this stage the fiber still preserved the original outline. However, as the grinding continued, the fiber was split into small pieces (Fig. 2). At this stage the fiber was first destroyed in the amorphous region and some crystal was also destroyed. Figure 3 (sample 3) shows that the fiber was crushed into very small pieces, especially in diameter; most of the fibers are smaller than 2  $\mu\text{m}$ , and in length sometimes they are around 5–10  $\mu\text{m}$ . Most of them seem to be needled powder. At this stage they still preserve some properties similar to a fiber, such as the orientation along the length, and we believe there are some small crystals in the powder.

### Thermal analysis

The TG curve and the DSC curve of the control sample (sample 0) and the smallest wool powder (sample 3) are shown in Figure 4 and Figure 5, respectively.



**Figure 2** Wool fiber ground for 0.5 h (sample 2).

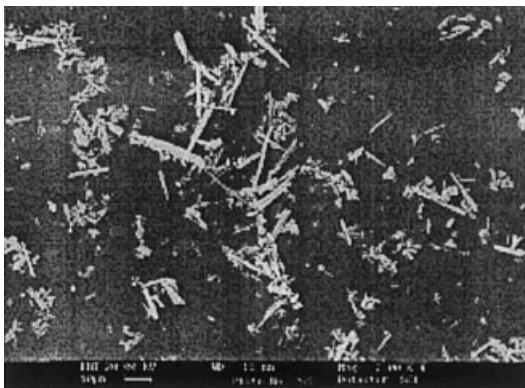


Figure 3 Wool powder ground for 3 h (sample 3).

There are four heat absorbing peaks in the DSC curves (also see Fig. 6), and they roughly correspond to two evident gravity losses. According to some researchers,<sup>12,13</sup> the four peaks can be explained as follows: peak 1 corresponds to the vaporization of bound water; peak 2 is ascribed to crystal cleavage (most evident in the control sample); and peak 3 corresponds to breakdown of crosslinks, such as —S—S— bonds, H bonds, salt links, which is denaturation; the high temperature of peak 4 corresponds to the rupture of peptide bonds, leading to the liquefaction (most evident in sample 2 and sample 3, and it shows a very strong single endotherm corresponding to liquefaction of the crystal at 294–316°C).

The intensity of peak 1 has a close relation to the quantity of the water (moisture) in the powder. Relative absorbed energy per unit weight (mg) is shown in Table I. As powder size decreases, the temperature at peak 1 increases; this shows the water-maintaining abilities of the wool powder of different sizes were also different. As the particle size decreased, the powder's affinity to water increased. This is perhaps be-

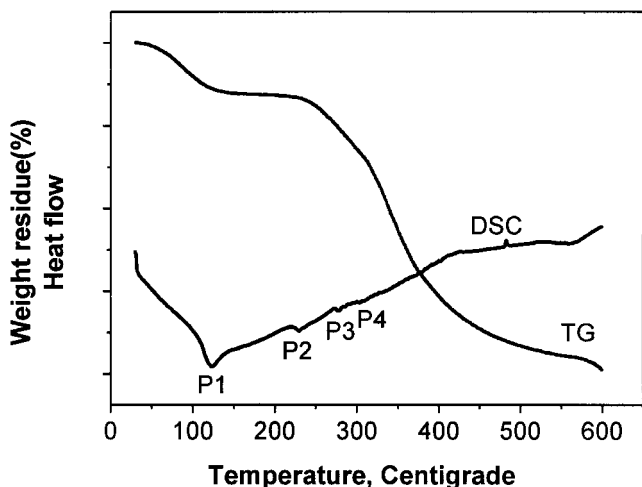


Figure 4 DSC and TG curves of sample 0 (control sample: wool fiber).

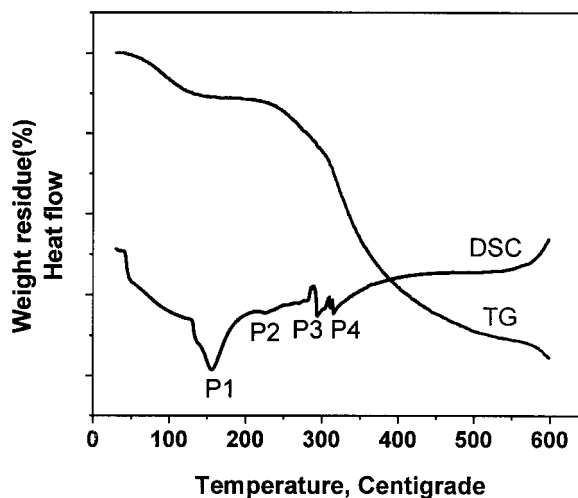


Figure 5 DSC and TG curve of sample 3 (the smallest powder).

cause the surface area of the powder was greatly increased, and at the same time the crystallinity was reduced and the moisture can go into the inner part of the material; thus its affinity to water was increased. Some articles have reported that the moisture regain usually cannot be totally evaporated if the temperature is lower than 150°C.<sup>14–17</sup> This can be more evidently seen in the ultrafine wool powder. In the control sample, the moisture can be evaporated under 120°C. However, in the smallest powder the moisture can only be evaporated around 150°C; the energy needed for removing the water was also higher than that of the larger particle powder. Another reason for the peak transferring from low temperature to high temperature is ascribed to the changes of the glass temperature of the powder. Some literature shows that around 160°C sometimes a new peak is generated in the wool fiber due to a glass transition occurring in the amorphous regions of the protein chains.<sup>12</sup> As the

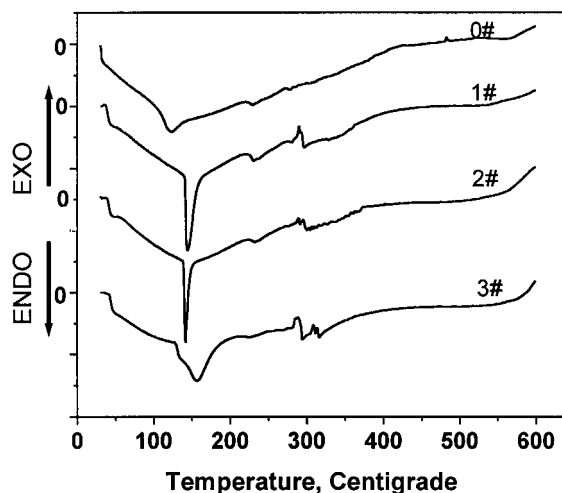


Figure 6 DSC curves of the four samples.

TABLE I  
Different Peak Temperatures in the DSC Curves of the Four Samples

Sample number	Weight (mg)	Relative absorbed energy in peak 1	Peak Temperature (°C)			
			Peak 1	Peak 2	Peak 3	Peak 4
0	3.88	1.00	122.8	226.5	277.6 (weak)	303.9 (very weak)
1	5.92	1.15	138.7	229.8	281.1	296.0
2	3.28	1.18	140.4	233.4	289.0	303.9
3	5.68	1.28	156.0	226.5	294.9	316.3

particle size decreases, the crystallinity is greatly reduced and the amorphous region is increased; thus the absorbed heat for glass transition also increases. These two peaks (water evaporation and glass transition) combine together to produce a wide peak, which is shown as peak 1 in Figure 2. The peak area was determined by the moisture content, the affinity of the water to the powder, and also the glass transition energy, as the crystallinity decreased, these all increased, thus induced increasing of the peak increased and the peak temperature transferring to high temperature.

Related studies<sup>12</sup> have been made by DTA on polypeptides and on wool. There was a broad endotherm around 230°C, and a small one around 245°C; the lower was ascribed to crystal cleavage, and the melting of  $\alpha$ -keratin. Above 250°C, the degradation was observed. In our studied results, the DSC curve of the control sample was very similar to these typical results and the endotherm above 250°C was very weak; this shows degradation was almost occurred under 250°C. However, as the powder particle size decreased, the heat absorbing peak at high temperature became wide and sharp.

The results also show that as the particle size decreased, intensity of peak 2 relatively decreased; however, the intensity of peak 3 and peak 4 increased evidently. Perhaps this is mostly due to the changes of the crystal and the reduction of the crystallinity. The disruption of the disulfide linkages of wool diminished the stability to heat, whereas reconstruction of the crosslinks by treatment with a special method (such as potassium cyanide) can restore the heat stability.<sup>13</sup> Mechanical action together with some water and chemicals perhaps can lead to reconstruction of the crosslinks and some changes of the crystal. As the literature has reported,<sup>14,15</sup> there are two different kinds of structure in the wool fiber: below 120°C, wool mostly consists of normal  $\alpha$ -keratin structure, and above 130°C, the fiber will contract in the length and show a  $\beta$ -keratin structure. This indicates that the structure of the  $\alpha$ -keratin pattern can transfer to the  $\beta$ -keratin structure. Dirorio et al.<sup>18</sup> have shown similar changes in wool fiber recrystallized at various temperatures and extensions from a molten state in LiBr solutions. Under a certain condition, the structure of

the fiber's  $\alpha$ -helices will also change as well as the mobility of molecular chain segments, which would certainly reduce the rigidity of the keratin structure. These all show that new crosslinks and crystal can be reproduced in different processing. Some changes in the DSC curves perhaps can be ascribed to these changes in the powder production.

As for peak 2 to peak 4, the control sample is very similar to the literature results.<sup>13</sup> However, as the particle size decreased, perhaps new crystal and new crosslinks was reproduced during the grinding in which the integrated effect of mechanical action and chemical action was imposed onto the powder. Disulfide bond reduction should increase the ease of elimination of H<sub>2</sub>S and decrease the temperature of liquefaction of wool. Crosslinking the reduced wool with  $-\text{S}-(\text{CH}_2)-\text{S}=\text{S}$  bridges is known to restore, and in fact, enhance the tensile strength of the wool fiber. It should also increase the thermal stability by diminishing the H<sub>2</sub>S, etc., thereby increasing the interchain bonding energy. Usually, thermal decomposition of wool may be expected from the following: (1) elimination of small molecules such as H<sub>2</sub>O, H<sub>2</sub>S, CH<sub>3</sub>SH, CO<sub>2</sub>, and NH<sub>3</sub>, from the reactive side chains of the continuant amino acids; (2) breakdown of the crosslinkages,  $-\text{S}=\text{S}=\text{S}$  bonds, H bonds, salt links; (3) by rupture of peptide bonds, leading to liquefaction. Increasing the intensity of peak 4 shows that decomposition of the wool became more difficult as the powder size decreased.

The TG curve shows that the fibers are similar to each other in weight loss during the elevated temperature. (See Fig. 7.) However, sample 3 shows evident high residue than other samples; weight of the residue of samples 0–2 were around 19%, and sample 3 remained around 20%. This confirms that during the long time processing for obtaining smaller wool powders, the loss of noncarbon elements in the formation such as H<sub>2</sub>S and NH<sub>3</sub> was greater than other samples of large particle size; thus the relative retained carbon elements were more than for other samples of large particle size. More relative carbon element in the smaller powder is another reason leading to the high thermal stability of the powder. High stability of the powder is a good virtue that can be utilized in the polymer polymerization and for the powder utiliza-

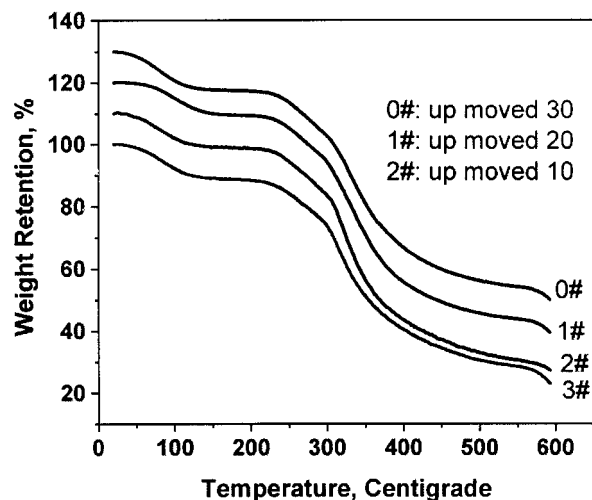


Figure 7 TG curves of the four samples.

tion in the coating of some materials under high temperature treatment.

### CONCLUSIONS

Wool fiber around 25  $\mu\text{m}$  in diameter can be crushed into fine powder; the diameter of the powder was mostly around 2  $\mu\text{m}$ , and the length was most around 5  $\mu\text{m}$ . TG analysis shows weight of the residues after 600°C increased as the wool powder particles size decreased. As the particles size decreased, the temperature for water evaporation also increased to around 150°C. The temperature for the crystal cleavages and the destroy of the crosslinks was also increased, especially the temperature for the liquefaction increased, this perhaps mostly due to new crosslinks and new

crystal was reproduced during the processing of the powder under high mechanical effect and the action of integrated chemical and temperature. Thermal stability of wool powder was improved after the treatment, that means the powder can be widely used under some high temperatures.

We are exceedingly grateful to the National Natural Science Foundation of China for supporting this research.

### References

1. Yao, J.; Masuda, H.; Zhao, C.; Asakura, T. *Macromolecules* 2002, 35(1), 6–9.
2. Lock, R. U.S. Pat 5,252,285, October 12, 1993.
3. Lu, X.; Akiyama, D.; Hirabayashi, K. *J Sericultural Sci Jpn* 1994, 63(1), 21–27.
4. Takeshita, T.; Ishida, K.; Kamiishi, Y. *Macromol Mater Eng* 2000, 283, 126–131.
5. Otoi, K.; Horikawa, Y. U.S. Pat. 4,233,212, November 11, 1980.
6. Tsubouchi, K. U.S. Pat. 5,853,764, December 29, 1998.
7. Freddi, G.; Tsukada, M.; Beretta, S. *J Appl Polym Sci* 1999, 71, 1563–1571.
8. Tanaka, T.; Tanigami, T.; Yamaura, K. *Polym Int* 1998, 45(2), 175–184.
9. Kawahara, Y.; Shioya, M.; Takaku, A. *American Dyestuff Reporter* 1996, 85(9), 88–91.
10. Pavlath, A.; Houssard, C.; Camirand, W. *Textile Res J* 1999, 69(7), 539–541.
11. Miyamoto, T.; Amiya, T.; Inagaki, H. *Kobunshi Ronbunshu* 1982, 39(11), 679–685.
12. Menefee, E.; Yee, G. *Textile Res J* 1965, 36(9), 801–812.
13. Falix, W.; McDowall, M.; Eyring, H. *Textile Res J* 1963, 33(6), 465–471.
14. Feughelman, M.; Mitchell, T. *Textile Res J* 1966, 36(6), 578–579.
15. Bendit, E. *Textile Res J* 1966, 36(6), 580–581.
16. Schwenker, R. *Textile Res J* 1960, 30(10), 800–801.
17. Haly, A.; Snaith, J. *Textile Res J* 1967, 37(10), 898–907.
18. Diorio, A.; Mandelkern, L.; Lippencott, E. *J Phys Chem* 1962, 66(9), 2096.